Title
EXCITATION METHODS FOR ENERGY DISPERSIVE ANALYSIS

Author
Jaklevic, Joseph M.

Publication Date
1978-06-01

Submitted to the CRC Press, Inc.,
for book to be published in 1979

EXCITATION METHODS FOR ENERGY DISPERSIVE ANALYSIS

Joseph M. Jaklevic

June 1978

Prepared for the U. S. Department of Energy
under Contract W-7405-ENG-48

DISCLAIMER

Submitted to the CRC Press, Inc.,
for book to be published in 1979.

LBL-7998

EXCITATION METHODS FOR ENERGY DISPERSIVE ANALYSIS

Joseph M. Jaklevic

June, 1978

Prepared for the U. S. Department of Energy
under Contract W-7405-ENG-48

Chapter 3

EXCITATION METHODS FOR ENERGY DISPERSIVE ANALYSIS

Joseph M. Jaklevic

Department of Instrument Techniques
Lawrence Berkeley Laboratory
University of California
Berkeley, California 94720

June 1978

I. INTRODUCTION

Many of the recent advances in the area of energy dispersive x-ray flourescence analysis (XRF) have been the result of innovations in the manner in which flourescence excitation is achieved. Traditional XRF methods employed x-ray tubes to produce continuum photon distributions which irradiated the sample to be analyzed. The resultant fluorescent spectrum was then analyzed using a very high resolution Bragg crystal spectrometer to sequentially measure the energy and intensity of characteristic x-ray lines.

The advent of semiconductor detector x-ray spectrometers presents new opportunities to improve upon the traditional wavelength dispersive x-ray fluorescence method. The high efficiency with which semiconductor detectors can measure a range of characteristic x-ray energies allows the use of less intense excitation sources. On the other hand, the somewhat poorer energy resolution of these detectors compared to crystal spectrometers requires that greater care be taken in maximizing the fluorescent signal relative to unwanted background x-rays. By careful consideration of these factors, it is possible to develop powerful analytical methods.

Some of the more important x-ray excitation methods which have become widely used in recent years include low-power x-ray tubes,[1,2] radioisotope[3,4] sources, polarized x-ray beams,[5,6,7] fine-focus electron-beam probes,[8,9] and heavy charged particle beams from accelerators.[10,11] Each method has particular advantages and disadvantages which determine its use in a particular application. The choice of a method depends on a number of factors including availability, cost, speed, accuracy, and detectability. In the present chapter, we will attempt to describe the various methods in sufficient detail that a meaningful comparison can be made.

II. GENERAL FEATURES OF X-RAY FLUORESCENCE EXCITATION

The fluorescence process can be visualized with the help of Fig. 3.1. The incident radiation from the excitation source interacts in the atoms of the sample and, in some cases, creates vacancies in the inner atomic shell of the element of interest. These vacancies in turn can de-excite with the emission of x-rays whose energies are characteristic of that particular atom. To the extent that these atoms are evenly distributed in a homogeneous matrix and provided that the incident radiation flux is uniform, the number of x-rays detected in the spectrometer is proportional to the concentration of that element.

In general, the probability that a particle in the incident radiation flux will interact with a given trace constituent and produce a useful fluorescence x-ray is rather small. Most of the excitation radiation continues through the sample until it interacts with the atoms which constitute the bulk of the sample matrix. These interactions often produce unwanted background x-rays which interfere with the measurement of fluorescence x-rays. In biological samples, the sample matrix is normally dominated by the lighter elements typical of hydrocarbon compounds. The interaction of the incident flux in the matrix can give rise to secondary x-ray distributions which constitute a continuous background in the flourescence spectrum. The ideal excitation source produces a minimum amount of the unwanted background radiation while at the same time efficiently and uniformly fluorescing those atoms in the atomic number range of interest. Since no method has proven ideal for all types of applications, the choice of an optimum excitation method involves an understanding of how these various factors operate in the case of each type of incident radiation normally employed in XRF.

A. Photon Excitation

This techniques involves the use of electromagnetic radiation (x-rays) with energies sufficient to create vacancies in the atoms whose concentration is to be measured. The radiation is normally obtained from either x-ray tubes or radioisotopes sources. In the former case, the radiation is the result of the interaction of an energetic electron beam with the anode material of the x-ray tube. In radioisotope sources, the radiation is due to gamma-ray or x-ray transitions which result from the radioactive decay process. The incident x-ray spectrum can be either continuously distributed over a broad energy spectrum or concentrated in a discrete series of lines.

Photons incident on the sample interact via the photoelectric effect to produce inner-shell vacancies which give rise to the fluorescent lines. The probability for vacancy production is greatest for photon energies immediately above the threshold for the ejection of the bound electron. The probability then decreases as the inverse cubic power of the energy of the incident photon as it is increased above this threshold. This energy dependence has important consequences when one wishes to analyze a wide range of elements using a single energy photon source since the sensitivity will vary proportionally.

The probability for vacancy production is normally expressed in terms of a cross-section per atom which can be interpreted as the effective area of that particular atom when measured by the interaction with a beam of particles. Figure 3.2 is a plot of the photoelectric cross section for a number of elements of interest as a function of photon energy.[12] It is important to note that, for a given incident energy, the cross-section for vacancy formation varies significantly for different elements. For example, using 10 keV photons, the probability

for excitation of an Fe atom is 6.6 times greater than for Al. This represents a factor of 20 on a mass basis since Fe is more dense.

In order to overcome this wide variation, it is sometimes desirable to either use a continuum of x-ray energies in the excitation spectrum or perform a series of fluorescence measurements using several discrete energy photon sources which span the atomic number range of interest.

The sensitivity of analysis with photon excitation depends not only upon the probability of fluorescence excitation but also on the relative probability for producing unwanted radiation which can interfere with the observation of the lines of interest. For samples consisting predominantly of lighter elements, the most serious problems arise from the scattering of the incident photons in the sample matrix. In addition to the photoelectric effect which is exploited to produce the characteristic fluorescence, photons can also interact in matter via elastic and inelastic scattering processes. In elastic scattering, the photons' direction of propagation is changed without any loss in energy. Inelastic scattering results in a change of direction and a loss in energy which is governed by the well-known Compton equation. In either case, the photons in the incident beam can be scattered into the detector resulting in unwanted events in the pulse-height spectrum.

The probability for such scattering events can likewise be described by a cross-section such as the dashed curves shown in Fig. 3.2 which are measured for the case of carbon. Curve a) is the elastic scattering cross-section, b) is inelastic. Although these cross-sections are several orders of magnitude less than the photoelectric cross section, the hydrocarbon matrix is normally present in abundance far greater than the trace element of interest. Choosing 10 keV radiation on a

sample of 10 ppm Fe by weight in a carbon matrix, the ratio of scattered to fluorescence x-rays would be approximately 500 to 1.

A better idea of the effect of scattering on the fluorescence measurement can be obtained by examining the idealized spectrum shown in Fig. 3.3. Here we consider a monoenergetic photon source incident upon a biological sample consisting of a light-element matrix containing several trace elements. The prominent peaks are due to scattering in the matrix; the highest energy peak represents elastic scattering; the other, broader peak reflects the angular spread over which the inelastically scattered photons were detected. The smaller peaks in the middle of the spectrum represent the fluorescent x-rays of interest.

The detectability of the spectrometer is determined by the ratio of the fluorescence peaks to the background beneath them. In this illustration, the background below this peak is due primarily to incomplete collection of the energy deposited by the large scatter peaks for some small fraction of events. Since this background is proportional to the scattered intensity, it is obvious that the sensitivity of the measurement is limited by matrix scattering of the incident radiation.

As noted earlier, the variation in sensitivity due to the energy dependence of photoelectric cross-section could be reduced by using a continuum of photon energies in the excitation spectrum. However, since a continuum excitation source would yield a superposition of spectra similar to that of Fig. 3.3 integrated over all energies in the incident photon distribution, it is obvious that a much higher background would result. Figure 3.4 is a spectrum calculated for the same sample but with continuum excitation such as might be obtained from an x-ray tube. Two extreme cases of scattering probability are shown.

The more uniform energy dependence of fluorescence intensity is achieved only with an accompaning loss in the minimum detectable amount of trace elements.

Most systems which attempt to achieve lowest possible detectable limits use a series of discrete excitation energies to cover a wide range of elements.[13] The exception to this rule is the very low energy region where comparable sensitivities have been observed with continuum excitation. A comparison of results obtained with several types of photon-excitation methods is contained in Reference 3.14.

B. Electron Excitation

Electron beams are attractive candidates for fluorescence excitation because of the ease with which they can be generated at energies appropriate for vacancy production. Conventional high-voltage supplies can be used with simple thermionic electron sources to produce milliampere beams at energies up to 100 keV or more. Virtually all of the x-rays used in biological applications are the result of electron beam interactions with x-ray tube anodes.

Electrons incident on a target interact principally by an electrostatic interaction with the orbital electrons of the target atoms producing ionization. The probability of such interactions is large and results in the electrons loosing their entire energy in a very short distance. For example, a 50 keV electron has a range of 5×10^{-4} cm in a W anode. Although the number of ionization collisions within this distance is very large, most of them occur in the outer electronic shells where the fluorescence energies are well below the x-ray regions.

Figure 3.5 is a plot of the cross-section for K-shell ionization as a function of electron energy for several elements.[15] The cross-sections exhibit a less abrupt threshold than that for photons. The maximum

cross section is achieved at an incident electron energy 3 to 4 times the K-shell binding energy. It is interesting to note that the magnitude of these cross sections are of the same general order of magnitudes as those shown for the photoelectric effect in Fig. 3.2.

In addition to the ionization process, electrons interact in matter via a continuous deceleration process which produces a continuous x-ray background. The deceleration occurs when an electron is deflected by the positive field of a nucleus and results in a continuous distribution of emitted x-ray energies up to the energy of the incident electron. This "brehmsstrahlung" spectrum is a serious limitation on the use of electrons for trace analytical work since it is produced in interactions with any element in the sample including the matrix. The spectrum can be described approximately by the expression:

$$dN(E) = 2.76 \times 10^{-6} \, Z \, \frac{(E_o - E)}{E} \, dE \qquad (3.1)$$

where dN is the number of photons between energies E and E + dE, and Z is the atomic number. A detailed examination of the signal/background ratio for electron excitation can be carried out using Eq. 3.1 together with appropriate electron range and ionization cross section data.[17]

Figure 3.6 is a schematic spectrum for the same hypothetical sample as was used in Figs. 3.3 and 3.4 but using 20 and 40 keV electrons. A quantitative comparison of this spectrum with the equivalent one for photon or heavy charged particle excitation demonstrates the poorer peak-to-background ratio evident in the electron excited spectrum. Electron beam excitation finds its most important x-ray fluorescence application when used in microprobe or scanning electron microscope applications. Here the relatively poorer sensitivity per unit volume is more than compensated by the ability to analyze very small areas. Since

elements are not uniformly distributed in many types of sample, the ability to excite extremely small volumes is a powerful analytical tool.

C. Heavy Charged Particles

Recently there has been an increase in the use of heavy charged particle beams such as protons (H^+) and alpha particles (He^{++}). Heavy charged particles exhibit large ionization cross-sections together with a much lower background relative to electrons. These beams are more difficult to produce than other forms of excitation; nevertheless, a number of facilities capable of generating several MeV beams of such particles are currently available for use in XRF and are supporting vigorous programs. Reference 3.10 contains the proceedings of a conference at which many of these programs were discussed.

The ionization cross sections for heavy particle excitation are similar to that of electrons with equivalent velocities. The property which makes their use attractive in XRF is the virtual absence of direct brehmsstrahlung rays. The mass of the nuclear particles relative to electrons reduces the effect of acceleration due to interactions with sample nuclei, and hence the probability of brehmsstrahlung production. The cross-section for continuum ray production is in fact proportional to the reciprocal of the square of the projectile masses, i.e., a proton produces 10^{-6} times less brehmsstrahlung than an electron. This results in a greatly enhanced peak-to-background ratio relative to electron-beam excited spectra.

Without the continuum background to obscure fluorescence peaks, it would appear that detectable limits for heavy charged particle excitation would be vastly reduced relative to other methods. However,

a second order process involving continuum radiation production by the energetic electrons ejected in the ionization process increases the detectable limit to a value similar to that of photon excitation.

Figure 3.7 is a plot of ionization cross-section as a function of energy for protons. The cross-sections are again comparable to those observed for other excitation methods but with a somewhat different energy dependence. The background sources can be understood by noting that the ionization cross-section is larger for light elements. For biological samples the majority of ionization events occur in a hydrocarbon matrix where the cross-sections are much greater than in the trace constituents. The maximum energy of the ejected electrons is approximately equal to the beam energy times the ratio of the mass of the electron to the heavy particle mass. These ejected electrons produce continuum x-ray radiation as they slow down in the matrix material as discussed earlier. This background constitutes the major limit of detectability for charged particle analysis. However, since it involves a second order process, the magnitude of the problem is far less severe than for direct electron excitation.

The spectrum in Fig. 3.8 is a calculated distribution using the same sample form as discussed in the previous comparisons. The continuum distribution is calculated assuming an ejected electron distribution appropriate for 3 MeV protons. The solid and dashed curves assume slightly different models for the continuum x-ray production and detection. What is most important are qualitative differences between this and the proceeding spectra. The shape of the background is similar to the continuum distribution for electron excitation but

with a lower end point energy and reduced intensity. The peak-to-background ratio is comparable to photon excitation but exhibits a different dependence on x-ray energy.

Inherent in the use of charged particle beams is the necessity for an electrostatic accelerator or cyclotron. Although it would not seem economical to build such a machine for analytical purposes only, there are a number of installations where these facilities exist and are available for part-time use in analytical programs.[10]

In addition to the inherently good sensitivity achieved with charged particles, there are numerous ways in which the focusing properties of the particles themselves can be used to advantage. For large area samples, it is possible to diffuse the beam over the entire sample resulting in a uniform excitation intensity. For small samples the beam can be focused to illuminate a small area or, in extreme cases, beams as small as 1 μm can be generated for use as microprobes.[19] One disadvantage is the need to operate with the sample in vacuum for most applications. However, there have been successful attempts to generate external proton beams for some applications.[20] By passing the beam through a thin foil into an He atmosphere at ambient pressure, it is possible to reduce target heating and charging effects and eliminate the inconvenience of vacuum operation.

III. X-RAY TUBES AND RAPID ISOTOPE SOURCES

A. X-ray Tubes

The most intense photon sources which are generally available are x-ray tubes. A beam of 50 kV electrons impinging on a target will generate approximately 10^{-5} photons per incident electron--for a 10 mA electron current this represents 6×10^{11} photons/sec or 20 Curies. These

photons are distributed between the characteristic x-rays of the anode material and the continuum brehmstrahlung distribution. This photon distribution can be used either directly or modified by external absorbers in order to produce more nearly monoenergetic radiation. The simplest way to produce a discrete energy spectrum is to place an x-ray transmission filter consisting of a thin (2.5×10^{-3} cm) foil of the anode material between the anode and the target. Since the characteristic x-rays of a given element have an energy immediately below the respective absorption edge energy, a foil of that element is a good transmission filter for those x-rays. A typical situation would be a Mo anode tube with Mo filtering resulting in a Mo $K_{\alpha,\beta}$ spectrum. This is a favorable situation for K-shell excitation of elements from Ca to Sr in the periodic table and for L-excitation of heavy elements such as Pb and Hg.

A more versatile scheme for obtaining discrete energy photon sources makes use of secondary fluorescence targets to transfer the output flux into the characteristic x-rays of the secondary target. Those x-rays in the tube output which are above the absorption edge of the secondary target are photoelectrically absorbed. The vacancies they create then de-excite with the emission of characteristic x-rays. Since the emitted x-rays are spatially isotropic, there is always a sizeable loss of photon flux in this two-step process. However, the use of external secondary targets allows one to easily change the excitation energy in order to optimize the sensitivity for measuring the element of interest.

The advantages of multiple excitation energies in photon excitation can be seen in Fig. 3.9. This is a plot of the relative efficiency for fluorescence x-ray production for a series of three fluorescent x-rays.

The advantage of having the incident energy immediately above the absorption edge of the element of interest is apparent. It is also possible to select against one element by choosing an excitation energy which is below the threshold for excitation.

Due to the inefficiency of the secondary fluorescence process, it is performed either in a very close geometry where the respective detector-sample-secondary target distances are small or, alternatively, a more powerful x-ray tube must be used. Reasonable counting rates have been achieved with less than 100 watts x-ray tube anode dissipation in the close-coupled case. X-ray tube powers of 1 kW or more can easily be achieved in the latter case if necessary.

Because of the normally isotropic distribution involved in x-ray production processes, x-ray excitation is well suited for large area samples, i.e., 1 to 10 cm^2. The ideal sample for x-ray excited fluorescence analysis is a thin, uniform and homogeneous sample. The thinness minimizes absorption effects particularly for lower energy flourescent x-rays. Uniformity and homogeneity ensure accuracy in the analytical results and facilitate corrections for absorption effect when necessary.

To the extent that the sample form departs from this idealized form, it may become necessary to perform corrections for matrix absorption and particle size effects. These both relate to the absorption of fluorescence x-rays due to thick, inhomogeneous or irregularly shaped samples that are problems normally encountered in x-ray analysis and extensive literature has been developed pertaining to methods for approximately correcting these effects.[21,22,23]

A number of intercomparison studies has established the validity of elemental analyses performed by this method.[24,25,26] In normal

everyday useage, it it possible to attain precisions and accuracies of analyses of 5% or less. In favorable cases, even better results are possible. The long-term calibration stability of such instruments is excellent and can easily be within the above precision.

B. Radioisotope Sources

An alternative source of photon excitation is achieved through the use of radioactive isotopes. There are a number of isotopes which emit a limited number of x-ray or gamma-ray lines suitable for fluorescence excitation. Their advantage derives from the cost and convenience of use. However, since the maximum source intensity easily available is of the order of 1.0 Curie, the fluorescence intensity is less than that achieved with x-ray tubes. In situations where thicker samples are available for analysis and where longer analysis times can be employed, the use of radioisotope sources can be advantageous. Table 3.1 is a partial list of suitable radioisotope sources and the associated radiation energies. Many of these sources are commercially available in geometries appropriate for XRF analysis.

The same criteria for sample form which applied in the case of x-ray tube sources apply also for radioisotopes. Particle size and matrix effects are also encountered and may be more difficult to handle due to the diffuse geometry of the source and the close source-detector geometry. Figure 3.10 are typical geometries employed in analysis. Figure 3.10a shows the case where the sample is directly excited by the radioisotope; 3.10b is a secondary-fluorescence geometry for variable energies. There have been attempts to exploit large area sources in order to produce a more uniform illumination of the sample and thereby reduce particle size effects. The inherent stability of isotopic sources

has the potential advantage of better precision and accuracy although in practice this advantage is seldom exploited.

Figure 3.11 shows spectra obtained from an identical sample of NBS orchard leaves using radioisotope excitation and using Mo x-ray tube excitation.[27] The spectra are similar although the x-ray tube spectrum exhibits a higher background due to scattered brehmsstrahlung. The radioisotopes used in the measurements were ^{109}Cd and ^{55}Fe. The difference in light element detectabilities using the two different excitation energies is qualitatively evident from the spectra.

It should be mentioned that radioisotope alpha-particle sources can be fabricated for certain applications. The intensity of such sources normally limits their use to the analysis of very light elements where the probability for ionization is large. An instrument using such a source has been constructed for used in the surface analysis of samples for very light elements. Figure 3.12 is a spectrum of a carbon film on a glass substrate obtained with an alpha-particle source operated in the same vacuum enclosure as the sample and detector.[28]

A number of references to energy-dispersive analysis using photon excitation are available. The reader is directed particularily to References 3.29, 3.30, and 3.31.

IV. CHARGED PARTICLES FROM ACCELERATORS, PROTONS, AND ALPHAS

Although the use of charged particle accelerators permits the use of a wide variety of projectile types and energies, developments in the field have centered on two principle methods of analysis. These typically use 3 MeV protons and 20 MeV alpha particles. An acronym commonly employed to described these methods is PIXE or Particle-Induced X-ray Emission Analysis.

The energies are chosen so that the endpoint of the ejected electron distribution results in a continuum distribution which does not interfere strongly with the x-ray region of interest.

Figure 3.13 is a diagram of a typical charged particle excitation apparatus.[22] The accelerated beam is directed down an evacuated beam line toward the target. Depending upon whether a line focus or diffused beam is required, adjustments in the magnetic focusing element upstream can be performed. A diffuser foil is employed before the sample in order to uniformly distribute the particles over the sample.

The samples are normally contained in multiple target holders to reduce the frequency of entry into the vacuum chamber. The beam passes through the thin samples and is stopped in an absorber shielded from the detectors field of view. In the case of Fig. 3.13, this is a graphite beam stop. The total current can be carefully measured and the result used to calibrate the yield of x-rays in the sample. X-rays are detected through a thin Be window in the side of the chamber.

In order to achieve optimal sensitivity in analysis thin substrates are used whenever possible. The range of 3 MeV protons in carbon, for example, is approximately 16 mg/cm^2, and the ionization process is most effective over the early part of the energy loss process. The thin substrate limits the amount of beam current which can be directed on the sample since local-heating in the non-conducting vacuum surroundings can evaporate the more volatile constituents or physically damage the sample. The use of conductive substrates such as thin carbon foils reduces the problem and also eliminates charging effects on the sample.

Figure 3.14 shows a series of spectra obtained on the NBS orchard leaf sample using a variety of excitation methods.[27] The reduced sensitivity for higher energy particles is primarily the result of the higher endpoint

energy for the continuum distributions. Most workers commonly employ protons at 3.5 MeV or less and alpha particles at 20 MeV or less.

Figure 3.15 is an example of several spectra of a bovine liver sample acquired at a series of incident proton energies. The differences between the two low energy spectra are due to the insertion of an absorber between the sample and detector to reduce the low energy counting rate and enhance the sensitivity for higher energy x-ray detection.

Types of samples which have been extensively studied by this method include thin-membrane air-particulate filters, ashed biological samples deposited on thin backings, thin sections of lyophilized tissues, and other similar types of samples.

The best accuracies and sensitivities are achieved with thin samples ($<1/mg/cm^2$). For thicker samples, corrections due to the energy loss of the incident protons and absorption of the fluorescence x-rays must be included. For thick biological specimens, electrostatic charging of the sample and possible evaporation of volatile contituents in the vacuum must be considered. Willis, et.al.,[33] discuss these problems and present comparisons of analyses obtained on standard materials prepared as both thick and thin samples.

The precision and accuracy obtained with charged particle excitation can be made comparable to other XRF methods in most cases of interest. Cablibration is normally performed using thin films of known weight to establish the sensitivity for a given element. For actual samples, corrections for proton energy loss and matrix absorption of the x-rays must be included. These are comparable to similar corrections for absorption effects using photon excitation.

A number of studies have compared photon excitation with charged particle excitation for precision, accuracy, and minimum detectable limits.[34,35,36]

Both methods are capable of analysis at concentrations of 1 ppm or greater and have an absolute particle limit of detectability in the range of 1 to 10 ngm/cm^2. The accuracies and precisions are more difficult to compare since it depends to a great extent on the sample form. For thin films, both can be made to perform at comparable accuracies. The choice of method in a particular application will depend upon other details and particularly on availability, convenience, and cost. For more extensive reading on the subject of charged-particle analysis, see References 3.37, 3.38, and 3.39.

V. ELECTRON BEAMS: MICROPROBES AND SCANNING ELECTRON MICROSCOPES

Direct excitation with electron beams is not routinely used on bulk specimens. The relatively poor sensitivity relative to other methods does not recommend its use. The principle application for electron excitation is in electron beam devices where the spatial resolution of finely focused beams is used to great advantage.

The two most commonly used electron beam devices are electron microprobes and scanning electron microscopes. Microprobes are characterized by higher beam currents (typically 10^{-6} to 10^{-9} A) and spatial resolutions of the order of 0.3 μm. They have been extensively used for quantitative analysis where the available beam currents make possible the use of wavelength dispersive spectrometry for analysis of elemental constituents.

Scanning electron microscopes (SEM) have significantly better spatial resolution (typically 0.01 μm (100 Å)) and operate at currents of 10^{-7} to 10^{-12} A. The normal mode of operation of one SEM utilizes a signal proportional to the intensity of secondary electrons emitted from the sample in order to generate a high resolution image of a portion of these samples. The electron beam is swept repeatedly across the specimen in a raster pattern while the secondary electron signal is synchronously displayed on a cathode ray screen.

The advent of semiconductor detectors with their inherently greater detection efficiency has permitted a simultaneous display of images extracted from individual characteristic x-ray intensities. It is thus possible to construct images of the elemental distributions of major constituents and relate them to the morphology of the specimen under study. The analysis of a particular area of the sample for several elements can be obtained by focusing the beam on a particular spot while a pulse height spectrum is accumulated. The sensitivity of such a measurement is limited by the contraints previously discussed; minimum detectable limits of less than 100 ppm for homogeneous samples are not practical.

The spatial resolution for x-ray images is not as good as can be obtained from secondary or backscattered electron images. X-ray signals can originate from anywhere within a volume surrounding the point of penetration of the electron beam, whereas backscatter images reflect only the surface layer where the beam enters.

Sample requirements are somewhat different for SEM and microprobe analysis. Since the most important information is related to the morphology of the particle, very little sample preparation is allowed. The sample is normally coated with a thin conductive layer of carbon in order to prevent distortion due to charging on the sample. The specimen must be capable of withstanding the the vacuum in the chamber without changing its composition.

High accuracies are normally not achieved in electron beam analysis particularly for samples such as biological specimens. The details of the electron beam loss together with the photon production and transport are not easily calculated. However, since most of the important information is contained in the relative spatial distributions of the elements, semiquantitative analysis is adequate in most cases.

Since the use of SEM techniques for the study of biological specimens is a highly developed technique for analysis, there are a number of review articles available for study. The reader is referred to the literature for more detailed information.[40,41,42]

VI. SPECIAL TOPICS

The previous sections dealt with variations in the application of XRF which are commonly employed and are likely to be available to the average user. There are several other variations of the method which are of additional interest either in special applications or because of their potential for future use. Several of these are discussed in the following section.

A. Proton Microprobe

Since charged particles beams can be focused, it is possible to combine the advantages of analytical sensitivity achieved in proton excitation with the spatial resolution available in microfocused beams. Several attempts to develop such a device have been made. Spatial resolutions of 2 μm have been achieved using a combination of fine collimators and magnetic focusing. Detection limits of a 1 to 10 ppm are possible for sample volumes of a few cubic micrometers. An interesting application of such a microprobe has been the measurement of the spatial distributions for several elements across the diameter of human hair.[19,43]

Although, photon excitation does not lend itself as readily to the production of fine focused beams, there have been attempts to develop small area analyzers using photon excitation. In one case, a crystal spectrometer is used to focus monochromatic radiation at a small line focus which then sees the sample.[44] In another method, a small collimator is placed on the detector in order to view an area of 1 mm diameter.[45]

B. Polarized X-ray Sources

The background observed in the case of photon excitation is proportional to the intensity of the primary beam scattered in the sample. One method of reducing this intensity takes advantage of the fact that the amplitude for scattering is zero in the same direction as the electric vector of the incident electromagnetic radiation. Most sources of protons are unpolarized, i.e., their electric vectors are randomly oriented. However, it is possible by successive scattering of an unpolarized beam to generate a beam in which the vectors lie in a specific direction perpendicular to the direction of propagation By placing the detector along this orientation, it is possible to minimize the amplitude of the scattered radiation. The photoelectric process, on the other hand, is insensitive to polarization and thus the fluorescence intensity is unaffected.

Several workers have demonstrated the expected reduction in background for a beam which had been partially polarized by successive scattering. The limitation on the widespread use of this technique is the inherent loss of intensity brought about the multiple scatter ing process.[5,6,7] Nevertheless, the technique has promise in the case of thick biological specimens.

C. Synchrotron Radiation

One method for obtaining intense, polarized beams is to use the radiation emitted by very high energy electron storage rings. There are a few facilities in the world where high-energy electron beam (3-5 GeV, i.e., 3×10^9 eV) are circulated in large diameter (~100 m) storage rings. As the electrons undergo the acceleration required to maintain the circular orbit, synchrotron radiation is emitted tangentially

to the orbit. This intense radiation is completely polarized, highly directional, and can extend to 30-40 keV in energy.

Using a crystal monochromator, it is possible to select a narrow energy band with which to excite samples. The polarization can be maintained while focusing a flux of 10^{11} photons/sec/mm^2 on the sample. This exceeds the capability of conventional x-ray tubes by a factor of 300. In one such series of measurements a minimum detectable limit of less than 10^9 atoms in small geological samples was achieved. This correspond to 10^{-12} grams of the element in question.[46,47]

D. Low Energy X-ray Detection

The applications of XRF which have been discussed emphasize the detection of elements above Z - 11. This is due to the inability of x-rays from lighter elements to efficiently penetrate the 2.5×10^{-3} cm Be window normally used in Si(Li) spectrometers. It has been shown, however, that by incorporating the spectrometer into the same vacuum system as the sample, it is possible to observe elements down to and including boron, E_k = 185 eV.[48]

Figure 3.12 shows the detection of carbon x-rays using alpha-particle excitation. Similar spectra can be obtained using electrons or protons for excitation. Photon sources are normally not used for light element excitation because of the source attenuation which they undergo.

Although the configurations used for such measurements are inconvenient, they demonstrate a significant capability for light element analysis particularly when used in conjunction with microprobe and heavy ion excitation. Although the detection of very light elements is of

dubious benefit in many biomedical applications, it is important to realize that Si(Li) spectrometers can be made capable of operation at these very low energies.

REFERENCES

3.1 Dyer, G. R., Gedke, D. A., and Harris, T. R., Fluorescence Analysis Using an Si(Li) X-ray Energy Analysis System with Low-power X-ray Tubes and Radioisotopes, Advances in X-Ray Analysis, Vol. 15, Heinrich, Barrett, Newkirk, and Ruud, Eds., Plenum Press, New York, 1972, page 228.

3.2 Jaklevic, J. M., Giauque, R. P., Malone, D. F., and Searles, W. L., Small X-ray Tubes for Energy Dispersive Analysis Using Semiconductor Spectrometer, Advances in X-Ray Analysis, Vol. 15, Heinrich, Barrett, Newkirk, and Ruud, Eds., Plenum Press, New York, 1972, page 266.

3.3 Zeigler, C. A., Ed., Applications of Low Energy X- and Gamma-Rays, Gordon and Breach Science Publishers, New York 1971.

3.4 Rhodes, J. R., Design and Application of X-ray Emission Analyzers Using Radioiosotope X-ray or Gamma-Ray Sources, Energy Dispersion X-Ray Analysis, ASTM Special Technical Publication 485, American Society for Testing and Materials, Philadelphia, 1971, page 243.

3.5 Kaufman, L. and Camp, D. C., Polarized Radiation for X-ray Fluorescence Analysis, Advances in X-Ray Analysis, Vol. 18, Pickles, Barrett, Newkirk, and Ruud, Eds., Plenum Press, New York, 1975, page 247.

3.6. Howell, R. H., Pickles, W. L., and Cafe, J. L., X-ray Fluorescence Experiments with Polarized X-rays, Advances in X-Ray Analysis, Vol. 18, Pickles, Barrett, Newkirk, and Ruud, Eds., Plenum Press, New York, 1975, page 265.

3.7 Dzubay, T. G., Jarrett, B. V., and Jaklevic, J. M., Background Reduction in X-ray Fluorescence Spectra Using Polarization, Nuclear Instruments and Methods, 115, 297, 1974.

3.8 Lifshin, E., Solid-State X-ray Detectors for Electron Microprobe Analysis, Energy Dispersive X-Ray Analysis; X-Ray and Electron Probe Analysis, ASTM STP 485, American Society for Testing and Materials, 1971, page 141.

3.9 Russ, J. C., Energy Dispersive X-ray Analysis on the Scanning Electron Microscope, Energy Dispersive X-Ray Analysis; X-Ray and Electron Probe Analysis, ASTM STP 485, American Society for Testing Materials, 1971, page 154.

3.10 Proceedings of the International Conference on Particle Induced X-ray Emission and Its Applications, Nuclear Instruments and Methods, Lund Sweden, 142, 1977.

3.11 Proceedings of the Third Conference on Application of Small Accelerators, ERDA Report CONF-741040, Duggan, J. L., North Texas State University, October 21, 1974.

3.12 McMaster, W. H., Kerr Del Grande, N., Mallett, J. H., and Hubbell, J. H., Compilation of X-ray Cross Sections, UCRL-50174, Lawrence Livermore Laboratory, 1970.

3.13 Jaklevic, J. M., Goulding, F. S., Jarrett, B. V., and Meng, J. D., Application of X-ray Fluorescence Techniques to Measure Elemental Composition of Particles in the Atmosphere, Analytical Methods Applied to Air Pollution Measurements, Stevens, R. K. and Herget, W. F., Eds., Ann Arbor Science Publishers, Ann Arbor, 1974, page 123, chap. 5.

3.14 Gedke, D. A. Elad, E., and Denee, P. B., An Intercomparison of Trace Element Excitation Methods for Energy-Dispersive Fluorescence Analyzers. X-ray Spectrometry, 6, 21, 1977.

3.15 Powell, C. J., Cross Sections for Ionization of Inner-shell Electrons by Electrons, Review of Modern Physics, 48, 33, 1976.

3.16 Green, M. and Cosslett, V. E., The Efficiency of Production of Characteristic X-radiation in Thick Targets of a Pure Element, Proceedings of the Physical Society, London, 78, 1206, 1961.

3.17 Jaklevic, J. M., Excitation Methods for Energy Dispersive Analysis, Proceedings ERDA X- and Gamma-Ray Symposium, Ann Arbor, 1976.

3.18 Garcia, J. D., X-ray Production Cross Sections, Physical Review A, Vol. 1, 1402, 1970.

3.19 Nobiling, R., Traxel, K., Bosch, F., Civelekoglu, Y., Martin, B., Poul, B., and Schwalm, D., Focusing of Proton Beams to Micrometer Dimensions, Nuclear Instruments and Methods, Vol. 142, 49, 1977.

3.20 Giauque, R. D., Goulding, F. S., Jaklevic, J. M., and Pehl, R. H., Trace Element Analysis with Semiconductor Detector X-ray Spectrometers, Analytical Chemistry, Vol. 45, 671, 1973.

3.21 Jenkins, R., An Introduction to X-ray Spectrometry, Heyden and Son, New York, 1974.

3.22 Birks, L. S., X-ray Spectrochemical Analysis, 2nd ed., Interscience Publishers, New York, 1969.

3.23 Leibhafsky, H. A., Pfeiffer, H. G., Winslow, E. H., and Zemany, P. D., X-ray, Electrons, and Analytical Chemistry, Wiley-Interscience, New York, 1972.

3.24 Camp, D. C., Cooper, J. A., and Rhodes, J. R., X-ray Fluorescence Analysis--Results of a First Round Intercomparison Study, X-ray Spectrometry, Vol. 3, 47, 1974.

3.25 Camp, D. C., Van Lehn, A. L., Rhodes, J. R., and Pradzynski, A. H., Intercomparison of Trace Element Determinations in Simulated and Read Air Particulate Samples, X-ray Spectrometry, Vol. 4, 123, 1975.

3.26 Alfrey, A. C., Nunnelley, L. L., Rudolph, H., and Smythe, W. R., Medical Applications of a Small Sample X-ray Fluorescence System, Advances in X-ray Analysis, Vol. 19, Gould, R. W., Barrett, C. S., Newkirk, J. B., and Ruud, C. O., Kendall-Hunt-Publishers, Dubuque, Iowa, 497, 1976.

3.27 Cooper, J. W., Comparison of Particle and Photon Excited X-ray Fluorescence of Environmental Samples, Nuclear Instruments and Methods, Vol. 106, 525, 1973.

3.28 Musket, R. G., KeVex Corporation, private communication.

3.29 Goulding, F. S. and Jaklevic, J. M., Photon-Excited Energy-Dispersive X-ray Fluorescence Analysis for Trace Elements, Annual Review of Nuclear Science, Vol. 23, 45, 1973.

3.30 Jaklevic, J. M. and Goulding, F. S., Energy Dispersion, X-ray Spectrometry, Herglotz, H. K. and Birks, L. S., Eds., Marcel Dekker, Inc., New York, 1978.

3.31 Woldseth, R., X-ray Energy Spectrometry, KeVex Corporation, Burlingame, California, 1973.

3.32 Willis, R. D. and Walter, R. L., private communication, 1978.

3.33 Willis, R. D., Walter, R. L., Shaw, R. W., and Gutknetht, W. F., Proton-Induced X-ray Emission Analysis of Thick and Thin Targets, Nuclear Instruments and Methods, Vol. 142, 67, 1977.

3.34 Jaklevic, J. M. and Walter, R. L., Comparison of Minimum Detectable Limits Among X-ray Spectrometers, X-ray Fluorescence Analysis at Environmental Samples, Dzubay, T. G., Eds., Ann Arbor Science, Ann Arbor, 1978, page 63.

3.35 Goulding, F. S. and Jaklevic, J. M., XRF Analysis--Some Sensitivity Comparisons between Charged-Particle and Photon Excitation, Nuclear Instruments and Methods, Vol. 142, 323, 1977.

3.36 Ahlberg, M. S. and Adams, F. S., Experimental Comparison of Photon- and Particle-Induced X-ray Emission Analysis of Air Particulate Matter, X-ray Spectrometry, Vol. 7, 73, 1978

3.37 Nelson, J. W., Proton-Induced Aerosol Analysis: Methods and Samplers, X-ray Fluorescence Analysis of Environmental Samples, Dzubay, T., Eds., Ann Arbor Science, Ann Arbor, 1977, chap. 2.

3.38 Johansson, T. B., Akselsson, and Johansson, S.A.E., Proton-Induced X-ray Emission Spectroscopy in Elemental Trace Analysis, Advances in X-ray Analysis, Vol. 15, Heinrich, Barrett, Newkirk, and Ruud, Eds., Plenum Press, New York, 1972, page 373.

3.39 Nielson, K. K., Hill, M. W., and Mangelson, N. F., Calibration and Correction Methods for Quantitative Proton-Induced X-ray Emission Analysis of Autopsy Tissues, Advances in X-ray Analysis, Vol. 19, Gould, Barrett, Newkirt, and Ruud, Eds., Kendall/Hunt Publishers, Dubuque, Iowa, 1972, page 511.

3.40 Electron Probe Microanalysis, Advances in Electronics and Electron Physics, Vol. 6, Tousimis, A. J. and Marton, L., Eds., Academic Press, New York, 1969.

3.41 Proceedings of National Conferences on Electron Probe Analysis.

3.42 Quantitative Electron Probe Microanalysis, Heinrich, K.F.L., Eds., NBS Publication, No. 298.

3.43 Cookson, J. A. and Pilling, F. D., Trace Element Distributions Across the Diameter of Human Hair, Physics Medical Biology, Vol. 20, 1015, 1975.

3.44 Ong, P. S. and Cox, Jr., H. L., Line-Focusing X-ray Monochromator for the Analysis of Trace Elements in Biological Specimens, Medical Physics, Vol. 3, 74, 1976.

3.45 Jaklevic, J. M., French, W. R., Clarkson, T. W., and Greenwood, M. R., X-ray Fluorescence Analysis Applied to Small Samples, Advances in X-ray Analysis, Vol. 21, Barrett, C. S., Leyden, D. E., Newkirk, J. B., and Ruud, C. O., Eds., Plenum Press, New York, 1978.

3.46 Sparks, C. J., et.al., Search with Synchrotron Radiation for Superheavy Elements in Giant-Halo Inclusions, Physics Review Letters, Vol. 38, 205, 1977.

3.47 Sparks, C. J., Ricci, E., Raman, S., Krause, M. O., Yakel, H. L., and Gentry, R. V., X-ray Fluorescence Analysis and Synchrotron Radiation, Fourth Annual Stanford Synchrotron Radiation Laboratory Users Group Meeting, SSRL Report No. 77/11, 1977, page 58

3.48 Musket, R. G., Detection of Proton-Induced Boron X-rays with a Si(Li) Detector, Nuclear Instruments and Methods, Vol. 117, 385, 1974.

Table 3.1

Radioisotopes for X-ray Fluorescence

Nuclide	Half-Life	Emission Energies
^{55}Fe	2.7 years	5.9 keV
^{109}Cd	453 years	22.1 keV, 87.7 keV
^{125}I	60 days	27 keV
^{241}Am	458 years	12-17 keV, 60 keV
^{57}Co	270 days	6.4 keV, 122 keV, 144 keV
^{238}Pu	86.4 years	12-17 keV

FIGURE CAPTIONS

Figure 3.1 Schematic diagram of the energy dispersive x-ray fluorescence method. Figure 3.1a shows geometry of excitation, sample, and detector; Figure 3.2a illustrates a simplified picture of the fluorescence process.

Figure 3.2 Cross section for K-shell vacancy production using photons for a few elements. The dashed curves show scatter cross sections for carbon. a) is elastic; b) is inelastic.

Figure 3.3 Schematic pulse height spectrum of a sample fluoresced with monoenergetic photons. The sample corresponds to elements present at the 10 ppm level in a hydrocarbon matrix.

Figure 3.4 Schematic pulse height spectrum of the same sample as used in Figure 3.3 but assuming continuum photon fluorescence.

Figure 3.5 Cross section for K-shell vacancy production using electrons.

Figure 3.6 Schematic spectrum of the same sample used for Figures 3.3 and 3.4 but using direct electron excitation.

Figure 3.7 Cross section for K-shell vacancy production using protons.

Figure 3.8 Schematic spectrum of hypothetical sample used previously but using 3 MeV proton excitation.

Figure 3.9 Relative probability for characteristic x-ray production for some typical secondary x-ray targets.

Figure 3.10 Geometries employed in radioisotope excitation.

Figure 3.11 Spectra of NBS orchard leaf standard taken with A) Mo x-ray tube excitation B) ^{109}Cd radioisotope source and C) ^{55}Fe source.

Figure 3.12 Spectrum of carbon film on a glass substrate obtained with an alpha-particle radioisotope source operated in the same enclosure as the sample and detector.

Figure 3.13 Diagram of a typical beam line for charged particle analysis. This particular system is in use at the Duke University.

Figure 3.14 Comparison of spectra obtained on NBS orchard leaf standard using several choices of charged particle excitation. Most workers commonly employ either protons in the 2 to 3 MeV range or alpha particles of 15-20 MeV.

Figure 3.15 Spectra of bovine liver specimens using a series of proton energies for excitation.

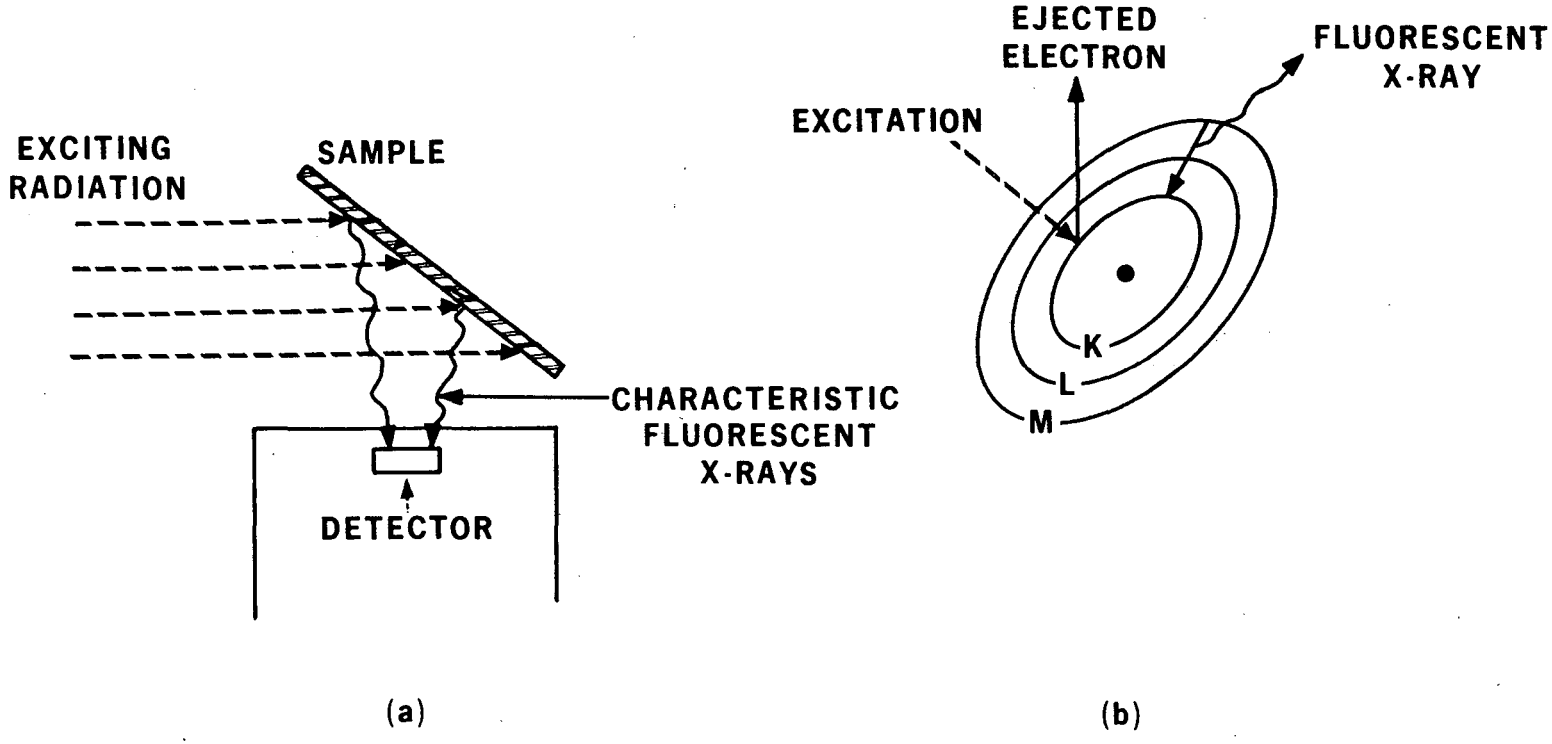
EXCITING
RADIATION
SAMPLE
CHARACTERISTIC
FLUORESCENT
X-RAYS
DETECTOR
(a)
EJECTED
ELECTRON
FLUORESCENT
X-RAY
EXCITATION
K
L
M
(b)

Fig. 3.1

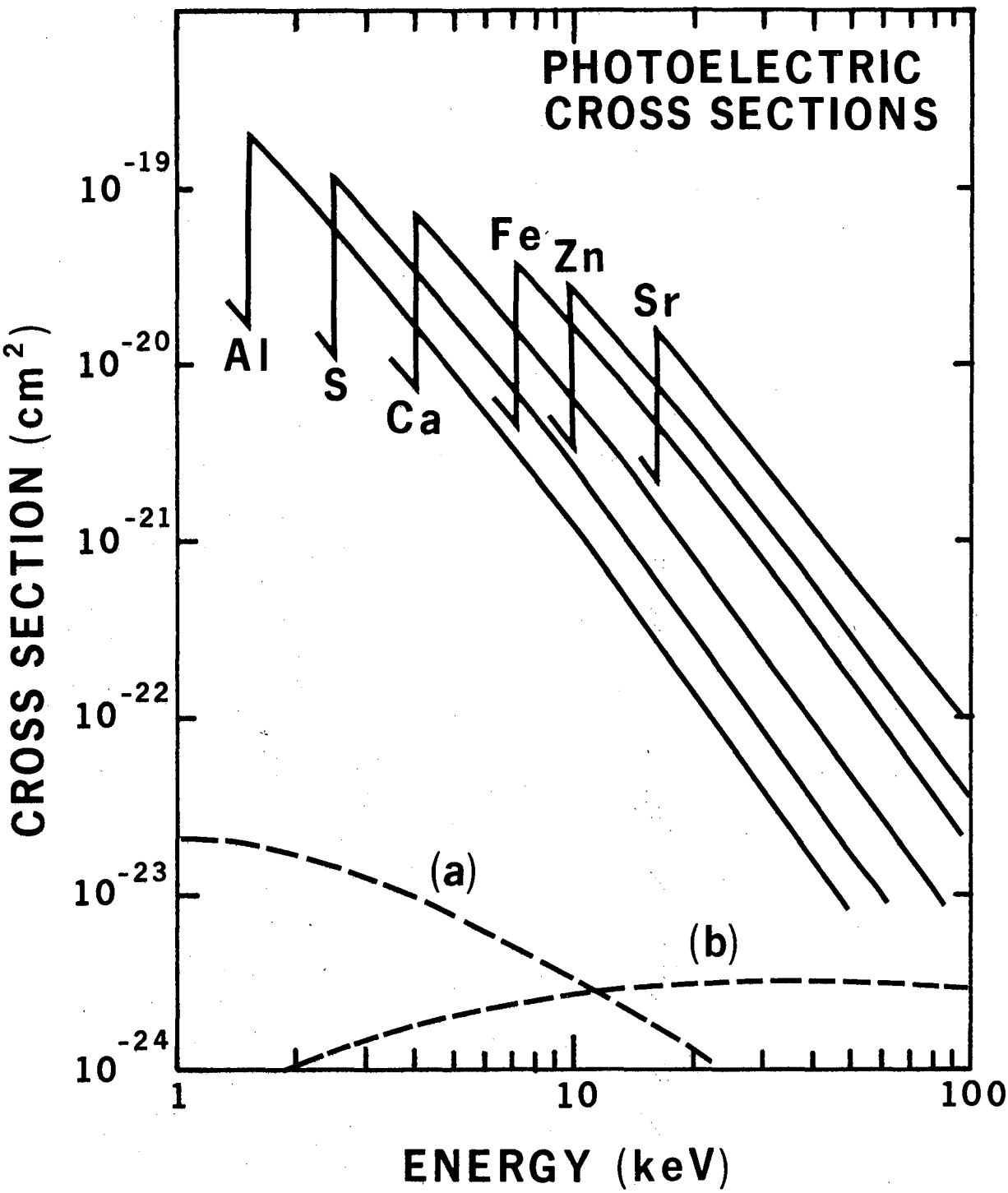

XBL 785-8849

Fig. 3.2

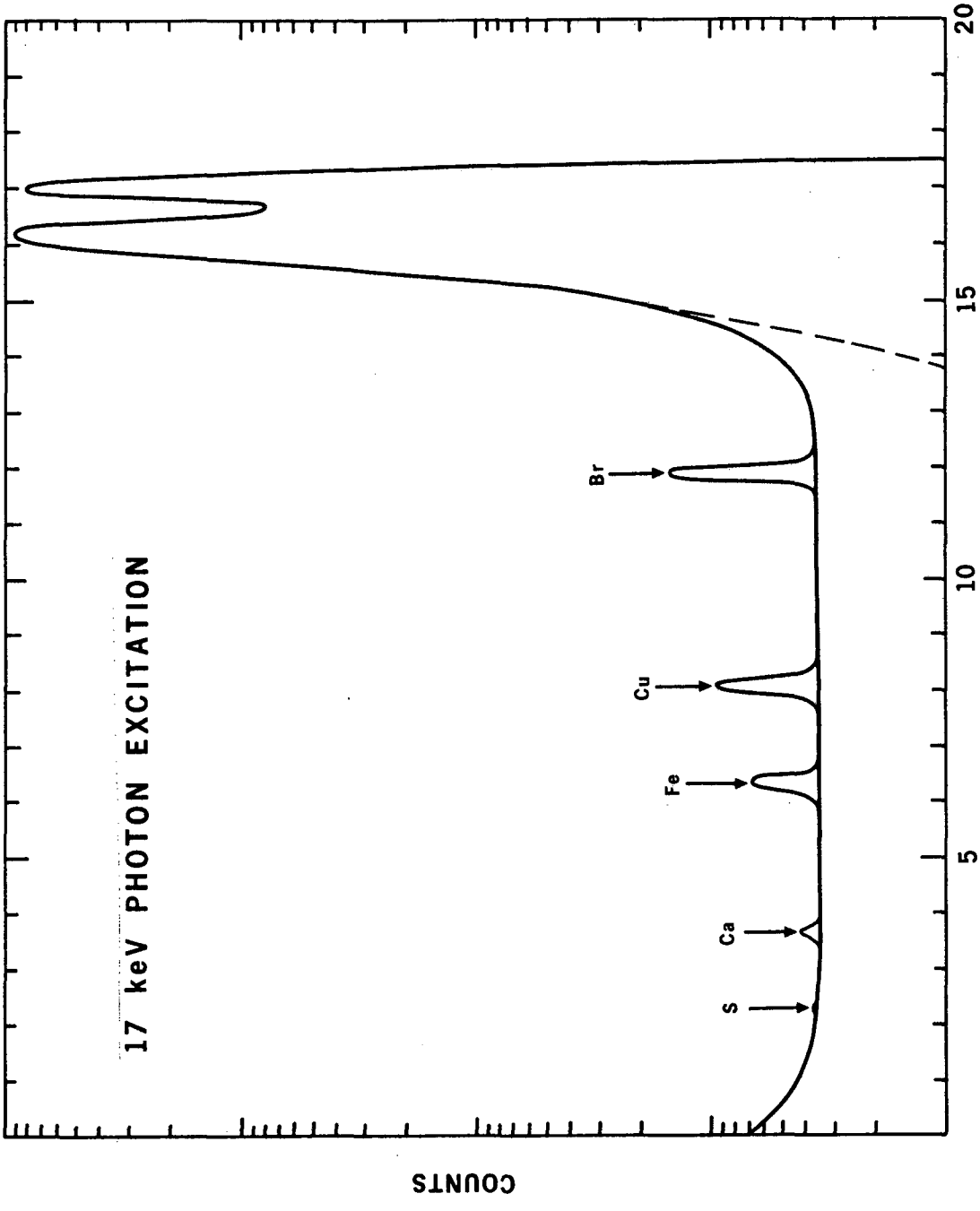

NBL 765-1671

Fig. 3.3

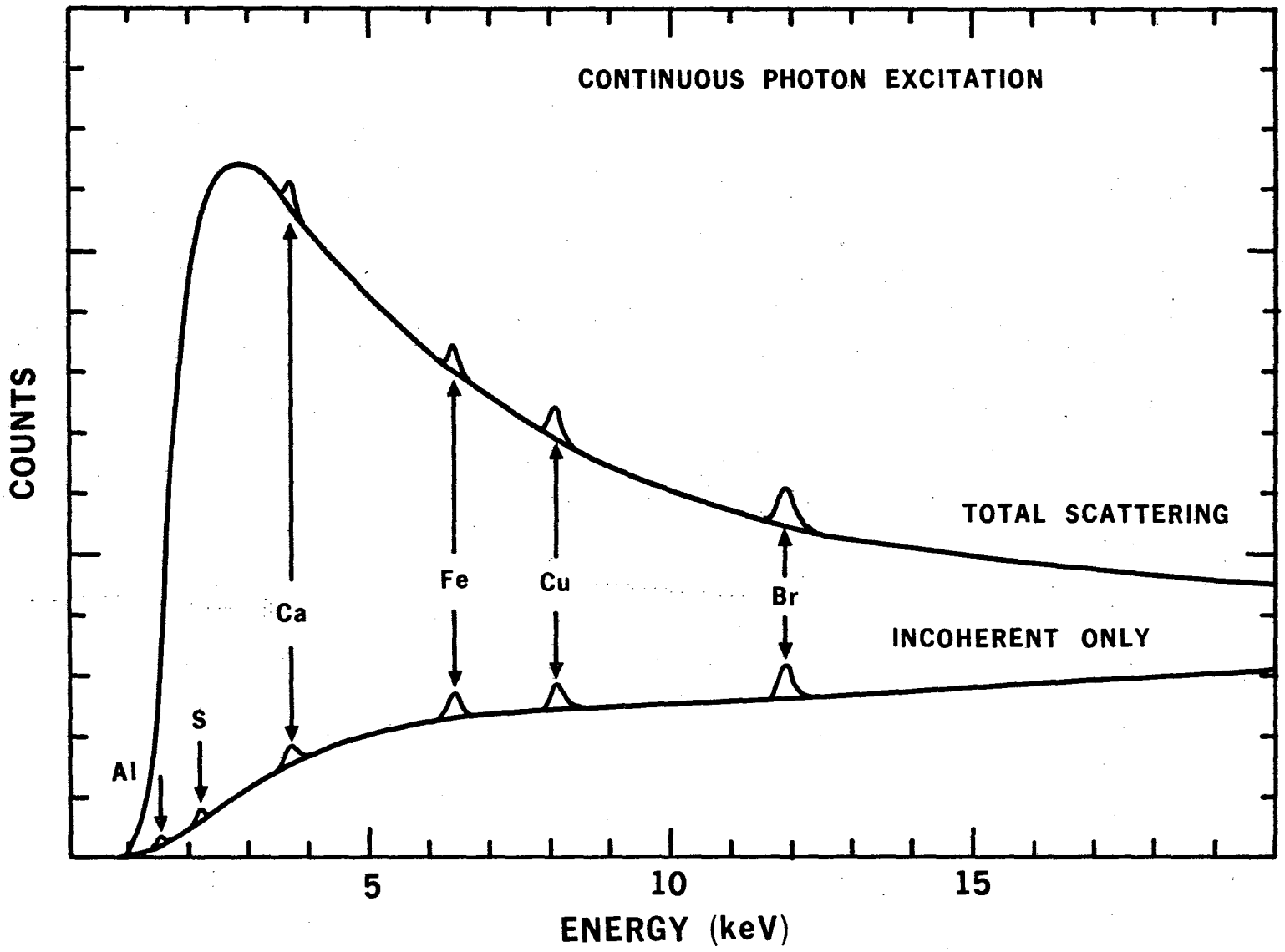

Fig. 3.4

XBL 765-1675

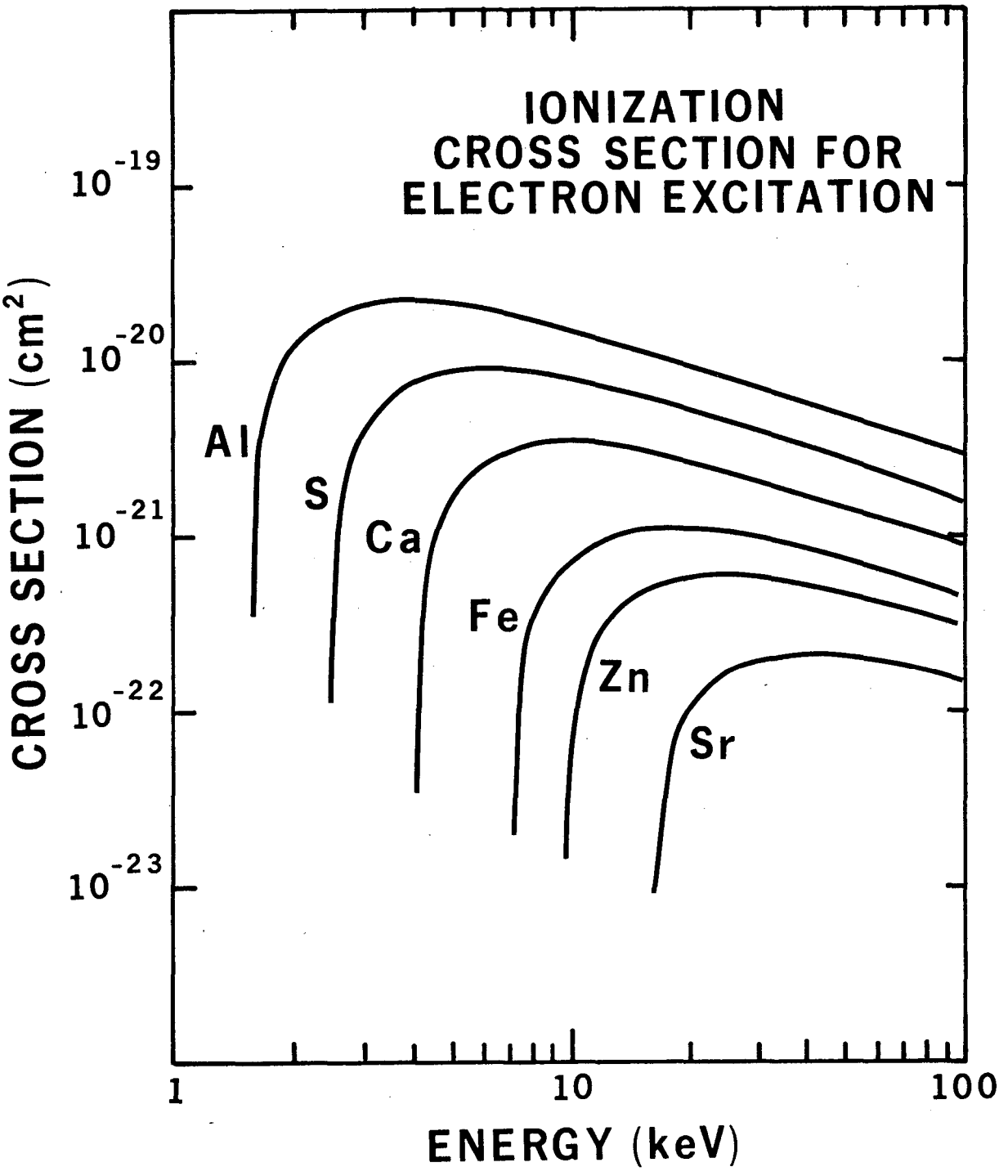

XBL 785-8850

Fig. 3.5

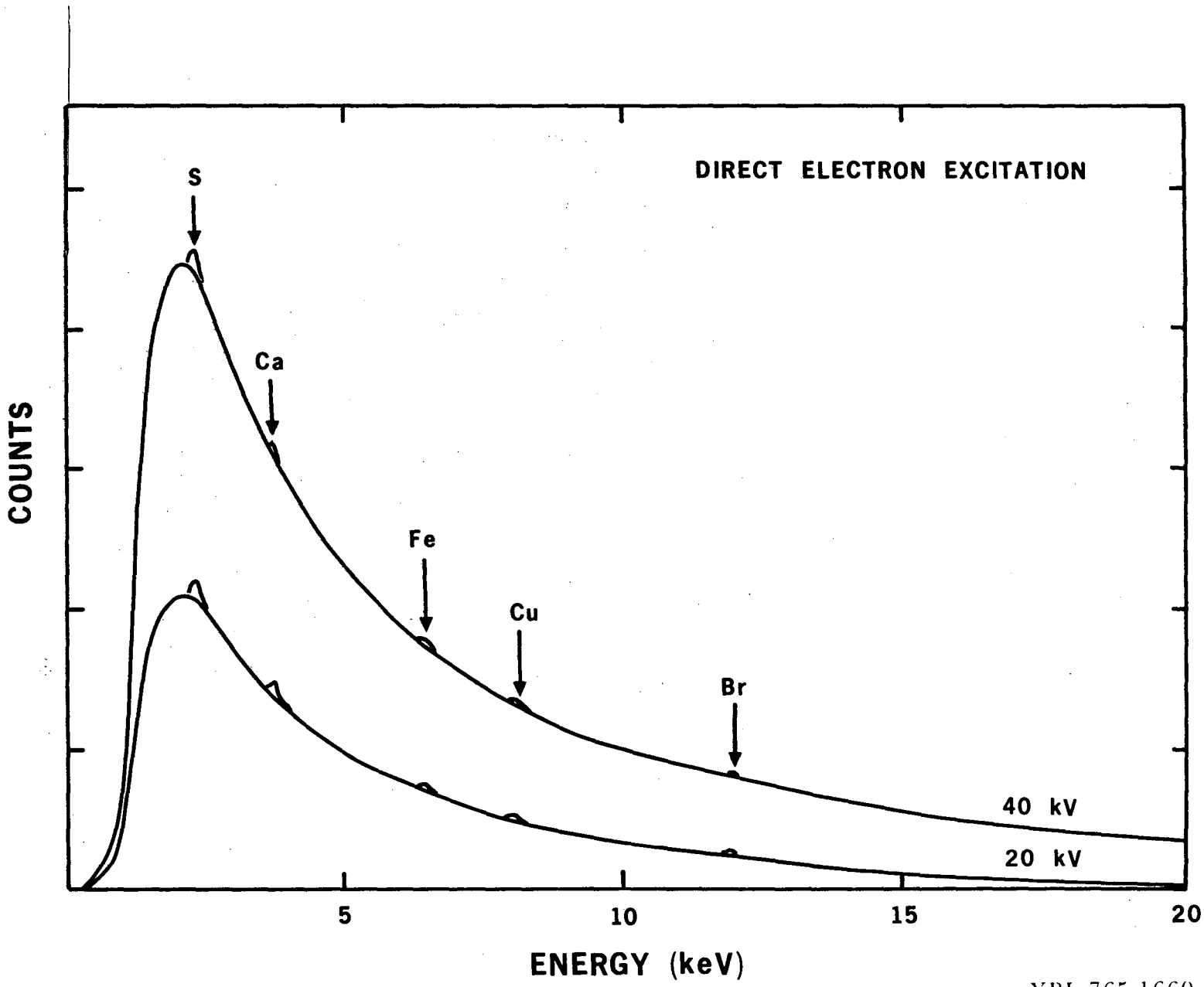

XBL 765-1660

Fig. 3.6

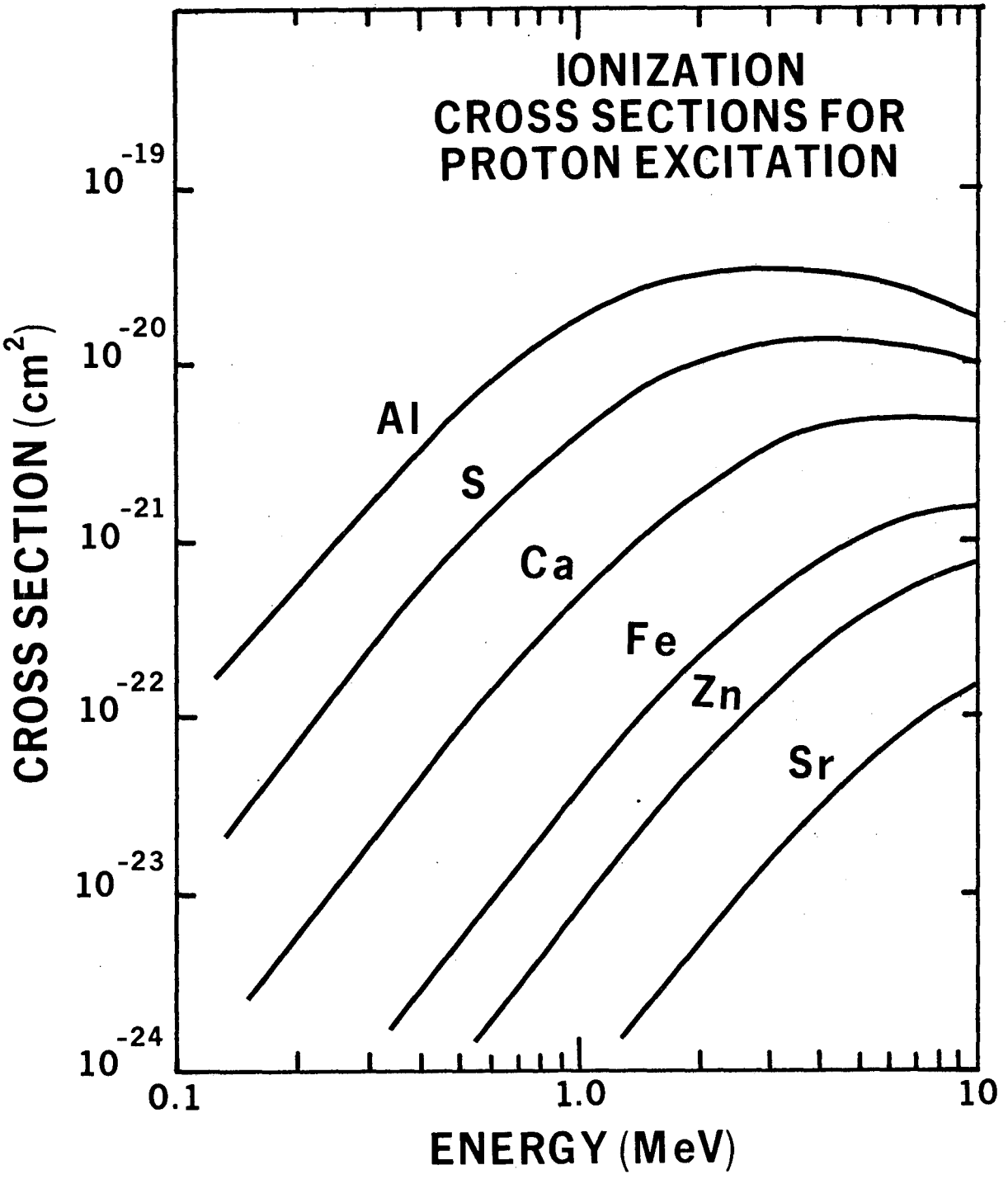

XBL 785-8851

Fig. 3.7

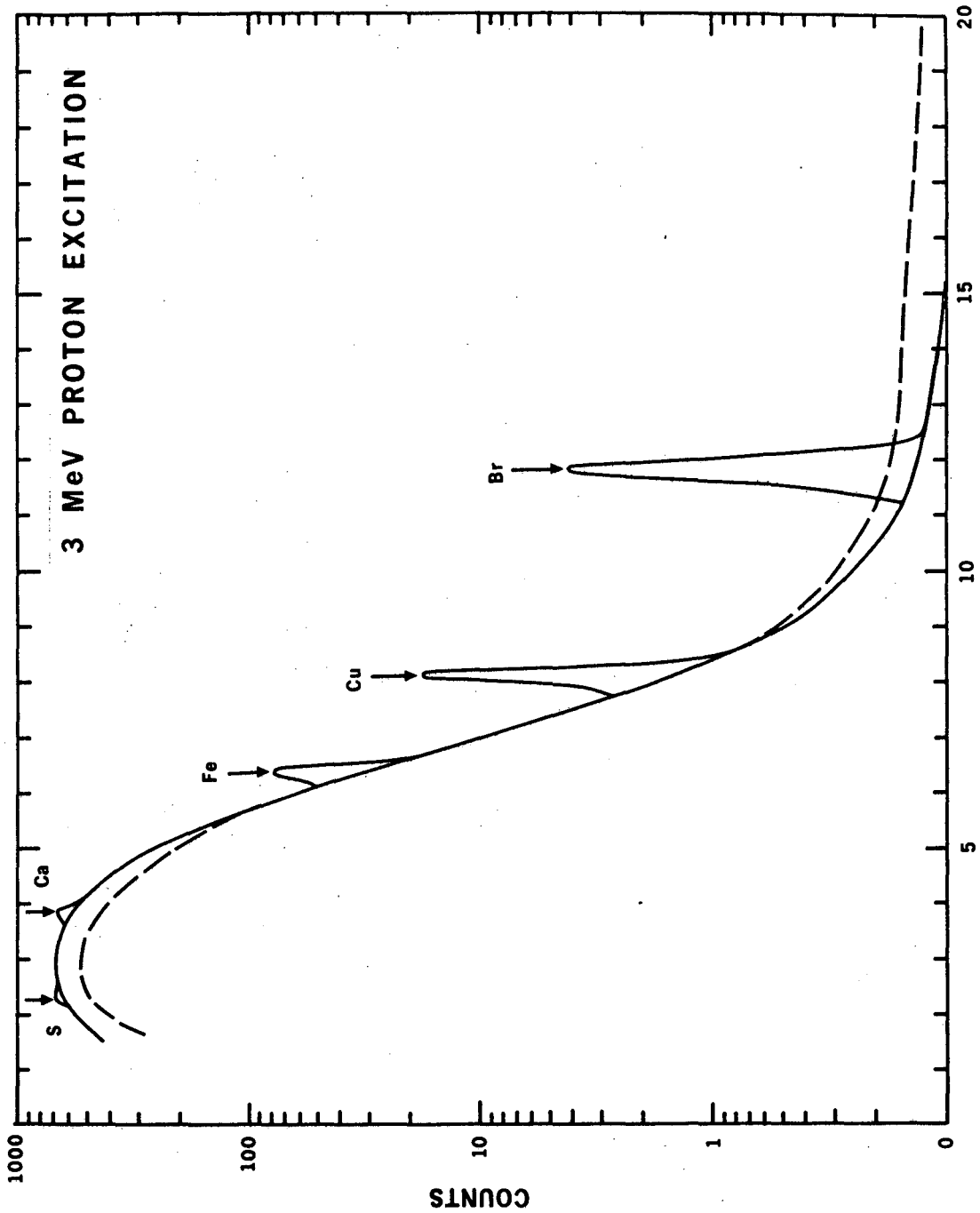

XBL 765-1661

Fig. 3.8

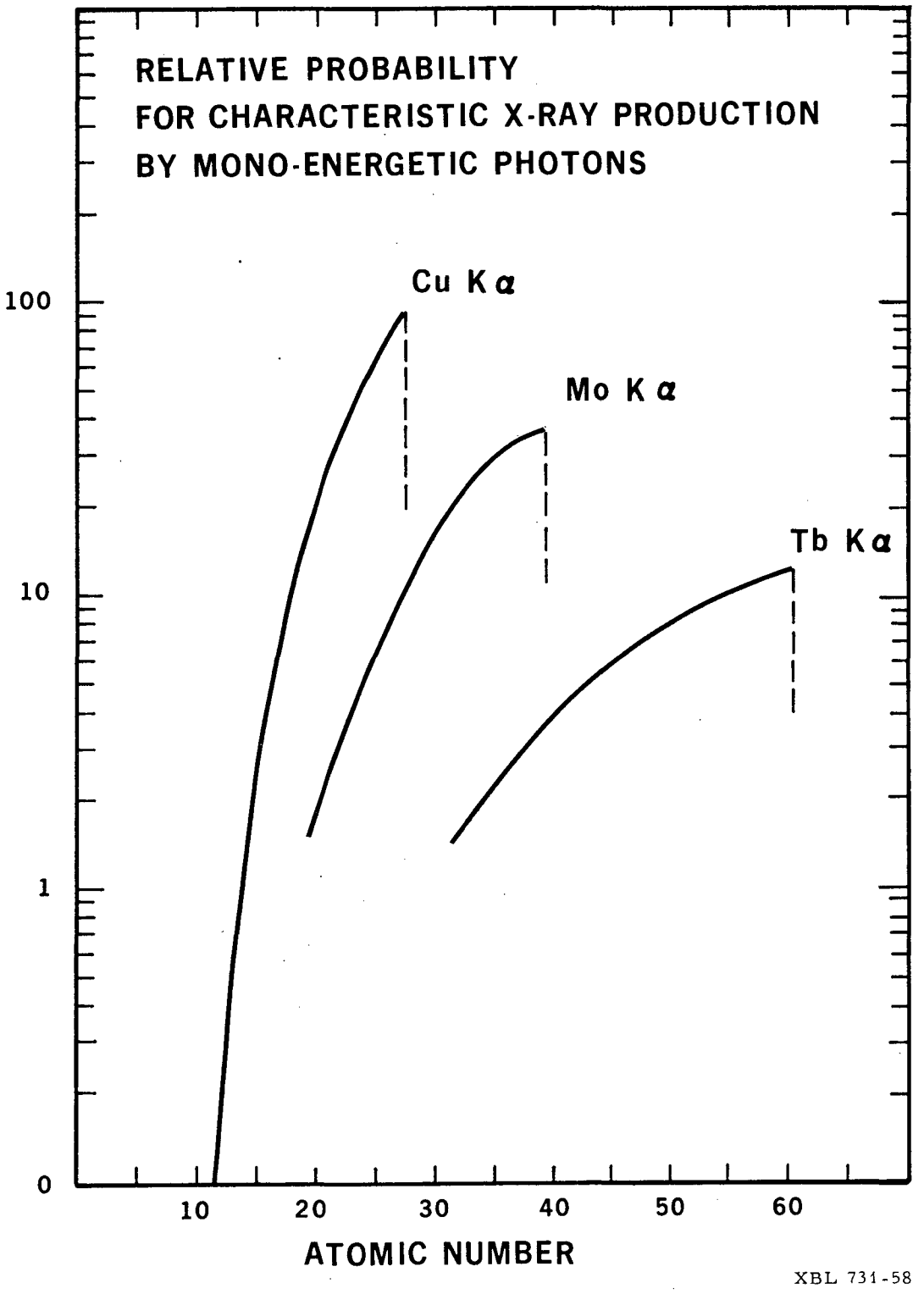
RELATIVE PROBABILITY
FOR CHARACTERISTIC X-RAY PRODUCTION
BY MONO-ENERGETIC PHOTONS
Cu Kα
Mo Kα
Tb Kα
100
10
1
0
10
20
30
40
50
60
ATOMIC NUMBER
XBL 731-58

Fig. 3.9

RADIOISOTOPE EXCITATION

A) DIRECT

B) SECONDARY FLUORESCENCE

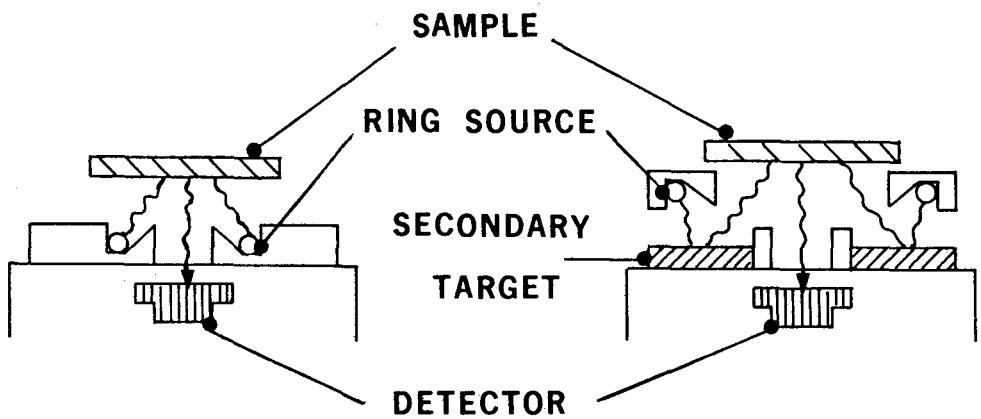

Fig. 3.10

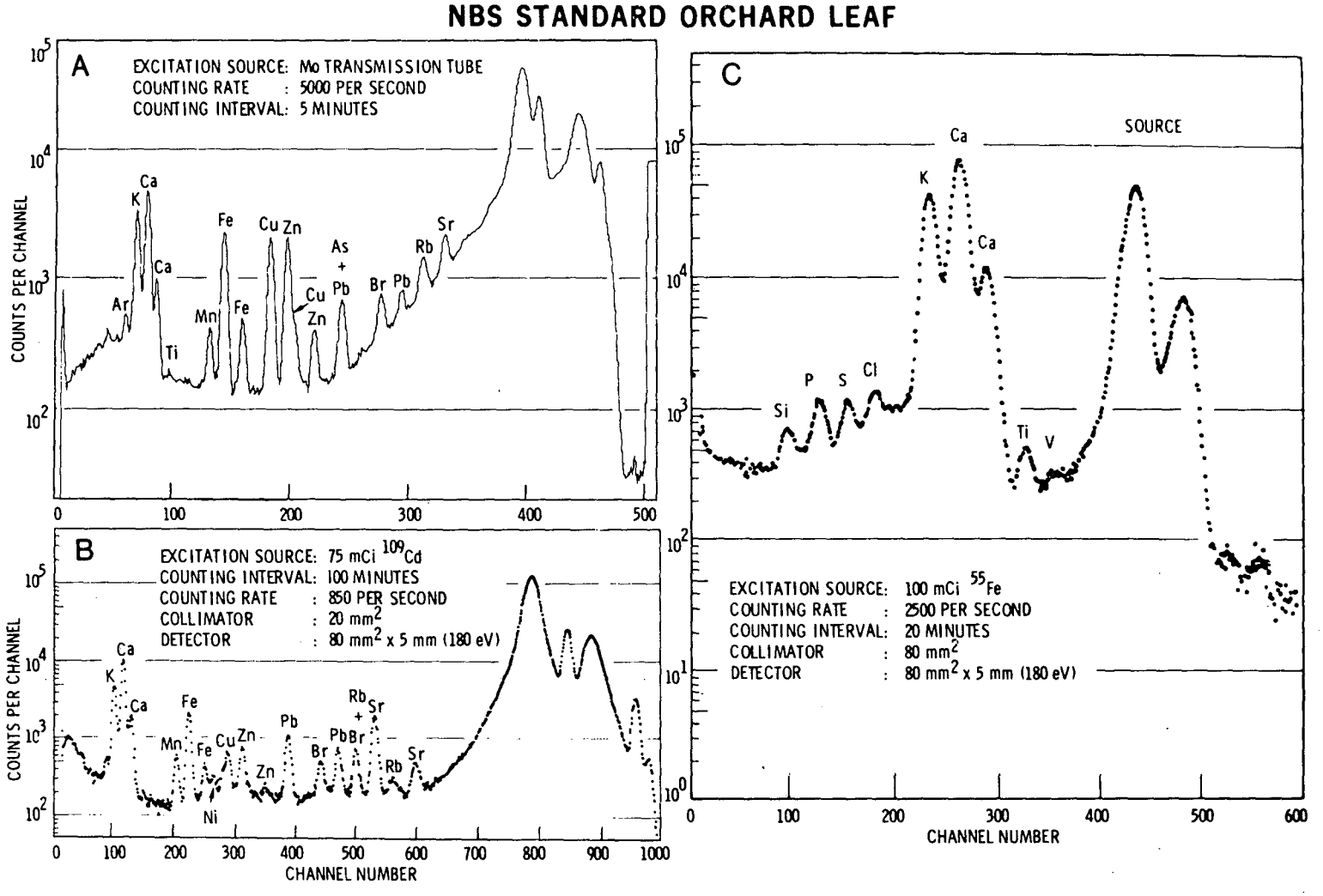
NBS STANDARD ORCHARD LEAF
A
EXCITATION SOURCE: Mo TRANSMISSION TUBE
COUNTING RATE : 5000 PER SECOND
COUNTING INTERVAL: 5 MINUTES
B
EXCITATION SOURCE: 75 mCi 109Cd
COUNTING INTERVAL: 100 MINUTES
COUNTING RATE : 850 PER SECOND
COLLIMATOR : 20 mm2
DETECTOR : 80 mm2 x 5 mm (180 eV)
C
SOURCE
EXCITATION SOURCE: 100 mCi 55Fe
COUNTING RATE : 2500 PER SECOND
COUNTING INTERVAL: 20 MINUTES
COLLIMATOR : 80 mm2
DETECTOR : 80 mm2 x 5 mm (180 eV)
COUNTS PER CHANNEL
CHANNEL NUMBER
XBL 785-8885

Fig. 3.11

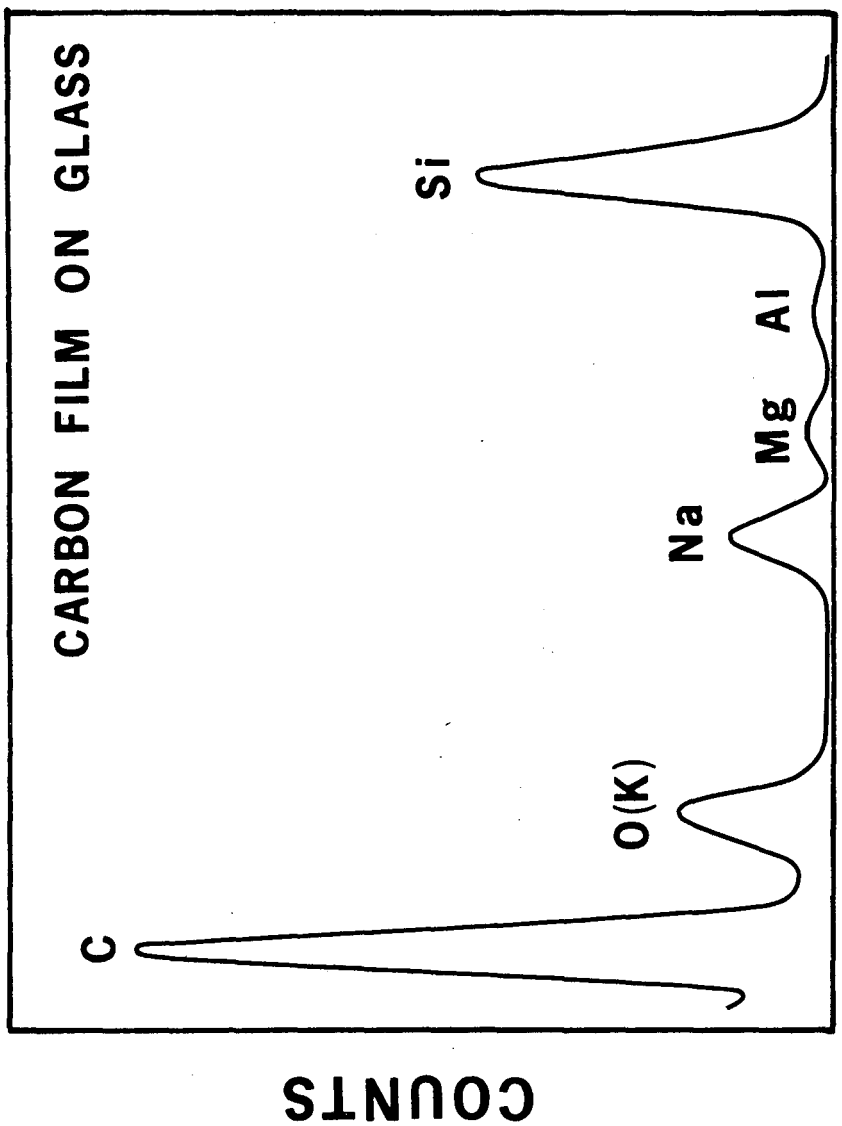

XBL 785-8852

Fig. 3.12

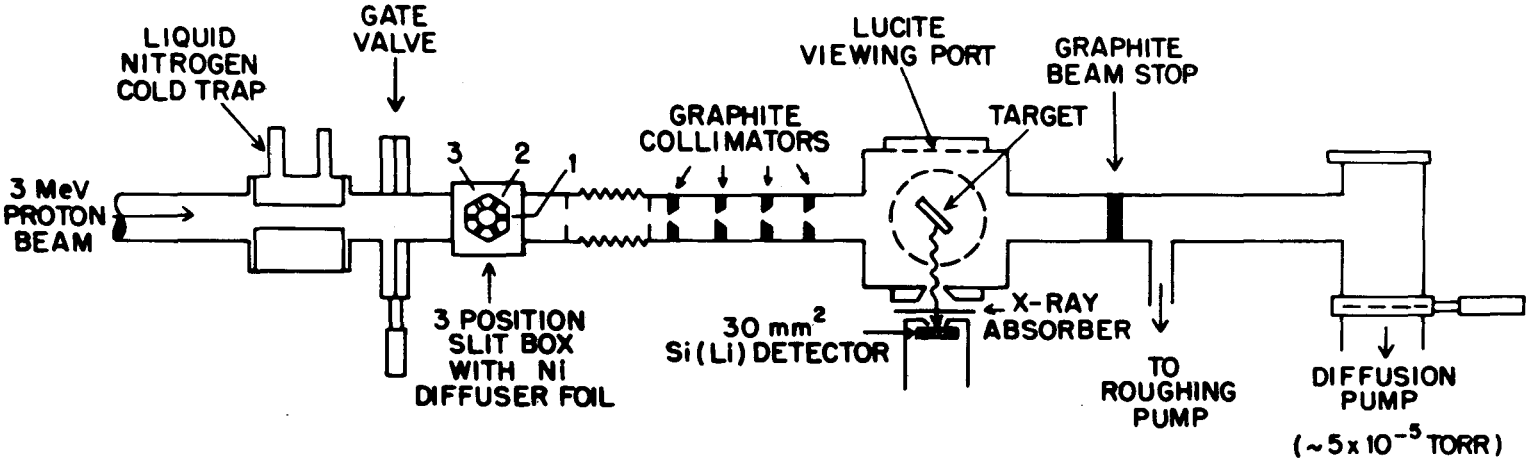

DIAGRAM OF EXPERIMENTAL BEAM LINE

Fig. 3.13

XBL 786-9324

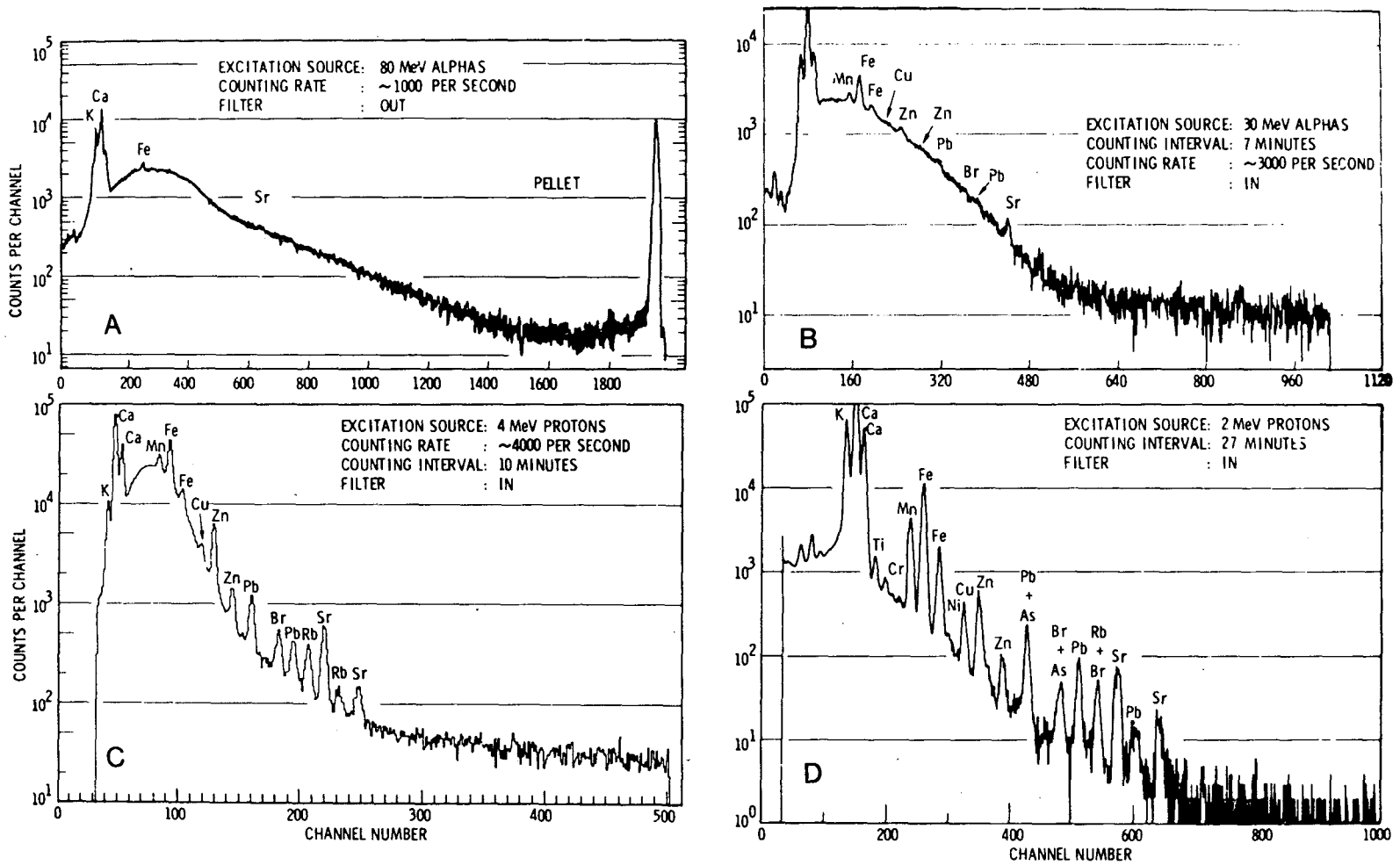

XBL 785-8884

Fig. 3.14

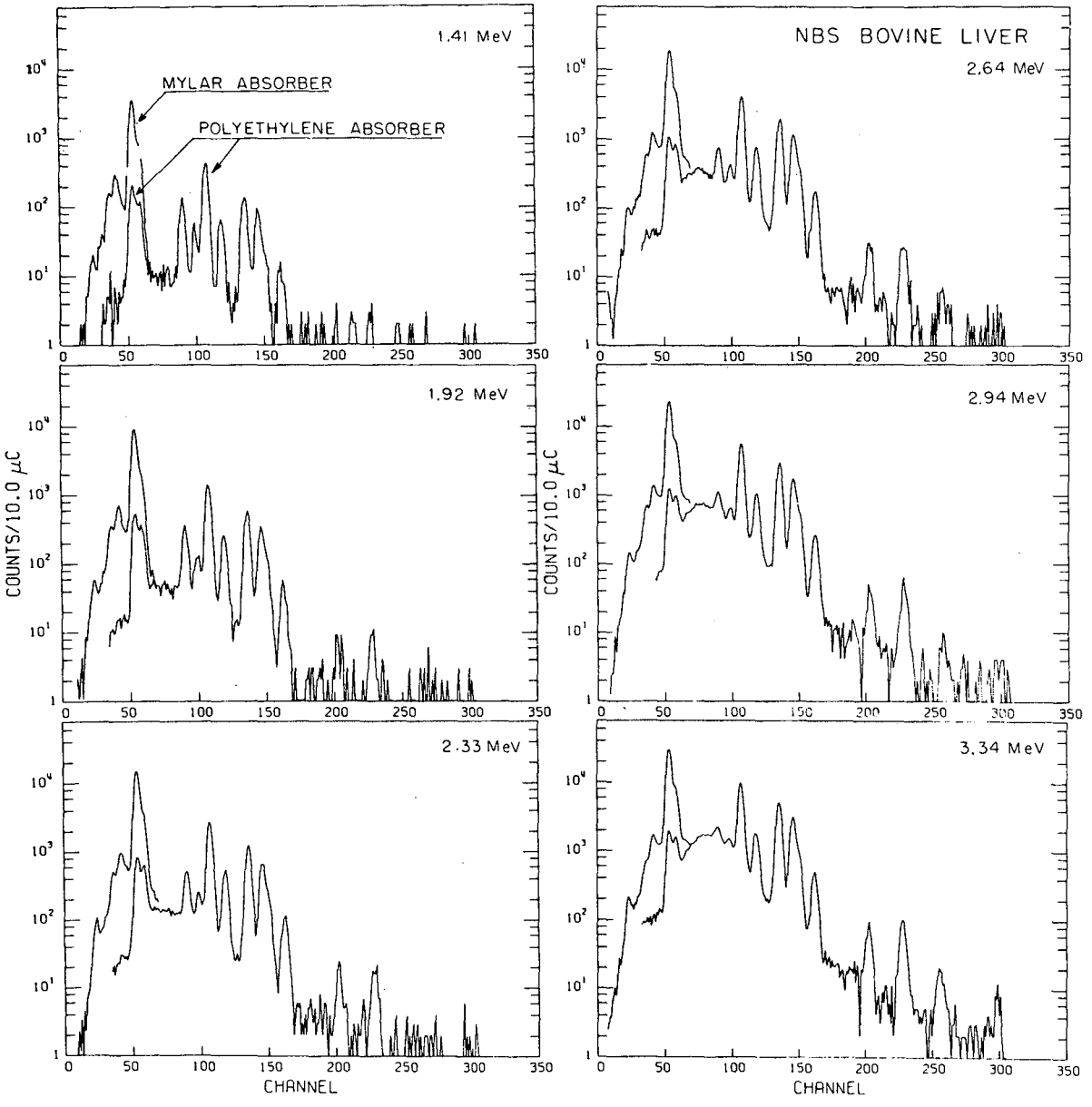

XBL 786-9328

Fig. 3.15

TECHNICAL INFORMATION DEPARTMENT
LAWRENCE BERKELEY LABORATORY
UNIVERSITY OF CALIFORNIA
BERKELEY, CALIFORNIA 94720